

Research Paper

A hook effect-free immunochromatographic assay (HEF-ICA) for measuring the C-reactive protein concentration in one drop of human serum

Jusung Oh^{1*}, Hyou-Arm Joung^{2*}, Hyung Soo Han³, Jong Kun Kim⁴, Min-Gon Kim¹✉

1. Department of Chemistry, School of Physics and Chemistry, Gwangju Institute of Science and Technology (GIST), Gwangju 500-712, Republic of Korea
2. Department of Electrical Engineering, University of California, Los Angeles, California 90095, United States
3. Department of Physiology, School of Medicine, Kyungpook National University, Daegu, Republic of Korea
4. Department of Emergency Medicine, School of Medicine, Kyungpook National University, Daegu, Republic of Korea

*These authors contributed equally to this work.

✉ Corresponding author: (M.G.K.) FAX: +82-62-715-3419, E-mail address: mkim@gist.ac.kr

© Ivyspring International Publisher. This is an open access article distributed under the terms of the Creative Commons Attribution (CC BY-NC) license (<https://creativecommons.org/licenses/by-nc/4.0/>). See <http://ivyspring.com/terms> for full terms and conditions.

Received: 2017.11.27; Accepted: 2018.03.23; Published: 2018.05.10

Abstract

The immunochromatographic (ICA) assay is a highly promising platform for rapid and simple detection of C-reactive protein (CRP) which is an indicator of the different phases of various diseases, as well as of inflammation and infection. However, the hook effect in the ICA assay limits the quantification of CRP levels at high CRP concentrations.

Methods: In this study, we developed a hook effect-free immunochromatographic assay (HEF-ICA) to detect CRP over a wide concentration range. The hook effect results from the simultaneous reaction of an excess target antigens with both immobilized and labeled antibodies respectively. To reduce the potential occurrence of this simultaneous reaction, we separated the migration of the target antigen and gold nanoparticle (AuNP)-labeled antibodies on a nitrocellulose membrane and analyzed the time profiles by modifying the ICA structure.

Results: The signal intensity of HEF-ICA was saturated at high CRP concentrations, without decreasing. The titration curve of HEF-ICA was adjusted with the Hill equation, and HEF-ICA was performed with the following parameters: limit of detection, 43 ng mL⁻¹; dynamic range, 119 ng mL⁻¹ to 100 µg mL⁻¹. The accuracy of the newly developed assay was evaluated using 33 clinical samples via comparison with a clinical chemistry analyzer.

Conclusion: HEF-ICA enabled the measurement of a wide range of CRP concentrations without the hook effect, and was suitable for point-of-care testing with fingertip blood sampling, as only a minute sample volume (2.5 µL) was required.

Key words: point-of-care testing, immunochromatographic assay, hook effect, C-reactive protein, wide range detection, minute sample volume

Introduction

C-reactive protein (CRP) serves as an opsonin in the initial phase of the immune response and enhances phagocytosis [1-3]. When infection and inflammation occur, CRP levels in human serum rapidly increase within a few hours and peak at 24-48 hours [4]. Therefore, CRP is mainly used as a biomarker of an infection or inflammatory process in

humans, with several thresholds (10-40 mg L⁻¹: mild inflammation or viral infection, 40-200 mg L⁻¹: active inflammation or bacterial infection, and over 200 mg L⁻¹: severe infection or trauma) [5, 6]. In addition, the pathogenesis of many diseases including cardiovascular disease, diabetes mellitus, metabolic syndrome, coronary syndrome, and atherosclerosis,

as well as diseases accompanied by infection and inflammation, shows a strong correlation with a wide range of serum CRP levels in humans [7-11]. Hence, prompt and continuous CRP detection and monitoring with quantitative analysis of a wide range of CRP levels is crucial for classification of the phases of the disease and inflammation stage, as well as for effective treatment [12-14].

Currently, immunoturbidimetric, immunonephelometric, radial partition immunofluorometric, and enzyme-linked immunosorbent assays are commercialized and mainly used as CRP assays. These assays are sufficiently practical to cover the range of CRP levels in the human body; however, they have some drawbacks including the multiprocessing step, necessity for skilled operators to ensure high reproducibility, and expensive equipment. These limitations render these assays inadequate for point-of-care tests (POCTs) [15]. Various new sensing platforms involving electrochemical or optical methods have been developed to meet the requirements of POCTs [16-18]. Among them, the immunochromatographic assay (ICA) is preferred for satisfying the requirements of a POCT, owing to its rapidity, cost-effectiveness, and user-friendliness. Nevertheless, the hook effect is still a major barrier in the detection of a wide range of CRP levels by ICA [19, 20]. The hook effect leads to false-negative results derived from a diminished or disappeared signal when a high concentration of the target antigen is input into the immunoassay without a washing stage. This hook effect results from simultaneous binding of excess target antigens to the immobilized and labeled antibodies respectively. In this reaction, the excess target antigens disturb the sandwich immunoassay on the test line and generate the false negative results despite a high input concentration of the target antigen [21].

Several studies have been conducted to overcome the hook effect of ICA. Leung et al. developed a barcode-style ICA to detect CRP with several test lines. This device's test line may diminish or disappear because of the hook effect; however, an additional test line can detect a broad range of CRP concentrations in a patient's sample via a semi-quantitative assay method without an additional sample preparation step [22]. Rey et al. detected a wide concentration range of CRP by a kinetic analysis and comparison of signal intensity between the test line and control line over time [23]. Oh et al. developed a three-line ICA strip that has an additional novel test line consisting of an antigen-antibody complex. By processing data on the signal intensity of the 3 lines of ICA, they were able to detect CRP in human serum in the range of 1 ng mL⁻¹

to 500 µg mL⁻¹ within 10 min [24]. Although these methods are based on novel approaches, they do not involve simultaneous quantitative and direct signal measurements.

In the present study, we attempted to develop a hook effect-free immunochromatographic assay (HEF-ICA) that can detect CRP in human serum directly. By adding an advanced paper-based structure to the conventional ICA strip, we controlled the timing of migration of the sample and gold nanoparticle (AuNP) conjugate. Consequently, the simultaneous reaction of excess target antigens with both antibodies was diminished and a sequential sandwich immunoassay was implemented. The new assay was modified such that it enabled measurement of the full clinical concentration range of CRP directly without the hook effect. Therefore, in the present study, we designed and characterized an advanced sensor structure and assessed its performance and specification with the conventional ICA. Further, we evaluated the accuracy and practicality of HEF-ICA by comparison with a conventional clinical chemistry analyzer, using 33 clinical samples.

Methods

Materials

CRP-free serum (90R-100), surfactant 10G (95R-103), and bovine serum albumin (BSA) were purchased from Fitzgerald Industries International (Acton, MA, USA). An anti-CRP polyclonal antibody (ab31156; "immobilized Ab") and a monoclonal antibody (ab10028, "labeled Ab") were obtained from Abcam Inc. (Cambridge, MA, USA). An anti-mouse IgG (M8642) was acquired from Sigma-Aldrich (St. Louis, MO, USA), whereas CRP (236608), laminated cards (HF000MC100) and a nitrocellulose (NC) membrane (HFB01804) were from Millipore (Billerica, MA, USA). The glass fiber pad (8964) and an asymmetric polysulfone membrane (ASPM, vivid plasma separation membrane, grade GX) were purchased from Pall Co. (Port Washington, NY, USA), and the sample pad (Grade 222) was sourced from Bore da Biotech (Gyeonggi-do, Korea). The gold colloidal solution was acquired from BBI International (EM.GC20; Cardiff, UK). Polyvinylpyrrolidone (PVP 29K), and other chemicals were from Sigma-Aldrich. All buffers and reagent solutions were prepared using distilled water generated using an ELGA water purification system (Lane End, UK). Fusion 5 was from GE Healthcare Life Sciences (Little Chalfont, UK). The 3D printer (3Dison multi) for manufacturing the cases for the ICA devices was purchased from Rokit (Seoul, Korea).

Preparation of the AuNP conjugate pad

The anti-CRP monoclonal antibody (10 μL , 1 mg mL^{-1} ; labeled Ab) was added to a mixture of 1 mL of 20 nm AuNP colloid (1 OD) and 100 μL of borate buffer (0.1 M, pH 8.4). After incubation at room temperature (RT; 25 $^{\circ}\text{C}$) for 30 min, 100 μL of BSA (10 mg mL^{-1}) was added to this mixture for blocking residual sites on the surface of AuNPs. After incubation at 4 $^{\circ}\text{C}$ for 60 min, the mixture was centrifuged in a refrigerated microcentrifuge (smart R17; Hanil Science Industrial Co., Gangwon-do, Korea) at 13,475 $\times g$ for 15 min at 10 $^{\circ}\text{C}$. The supernatant was discarded, and the AuNP conjugates were resuspended in 10 mM borate buffer (pH 8.4). The centrifugation and resuspension steps were repeated twice. The final resuspended AuNP conjugate solution was concentrated 10-fold by changing the solution volume. The (10-fold) concentrated AuNP conjugate was diluted with solution of the same volume containing PVP (20 mg mL^{-1}) and surfactant 10G (10 mg mL^{-1}). Two-fold diluted AuNP conjugate (10 μL) was loaded onto the glass fiber pad (0.4 \times 0.4 cm^2) and dried in a chamber with constant temperature and humidity for 15 min at 37 $^{\circ}\text{C}$.

Preparation of the ICA strip

Conventional ICA

The conventional ICA strip was assembled from an NC membrane, absorbent pad, conjugate pad, and sample pad. An anti-CRP polyclonal antibody (immobilized Ab) and anti-mouse IgG antibody were immobilized (8 and 4 mm from the top side of the NC membrane, respectively; 30 \times 2.5 cm^2) using a dispenser (DCI 100; Zeta Corporation, Kyunggi-do, Korea). The NC membrane loaded with two antibodies was dried in a chamber with constant temperature and humidity for 15 min at 37 $^{\circ}\text{C}$. After incubation, the absorbent pad (Grade 222; 30 \times 2 cm^2) was attached to the top side of the NC membrane with a 2 mm overlap. The combination of the NC membrane and absorbent pad was cut into 4 mm wide strips in a cutting machine. The conjugate pad and sample pad (Grade 222; 2 \times 0.4 cm^2) were attached to the bottom of the NC membrane with overlaps of 1.5 and 2.5 mm, respectively.

HEF-ICA

The NC membrane of HEF-ICA has a disconnected gap of 1.8 mm that is approximately 8 mm from the far end of the top NC membrane. This disconnected gap divides the top and bottom sections of the NC membrane, which are 0.8 and 1.5 cm length, respectively. The sample pad (Fusion 5; 0.4 \times 0.4 cm^2) was located on the disconnected gap in the NC

membrane, and the absorbent pad and buffer pad (Grade 222; 2 \times 0.4 cm^2) were fixed to the top and bottom sections of the NC membrane, respectively, with 2 mm overlaps. The intermediate pad (Fusion 5; 0.4 \times 0.5 cm^2), ASPM (grade GX; 0.4 \times 0.5 cm^2), and conjugate pad loaded with the AuNP conjugate (glass fiber 8964; 0.4 \times 0.4 cm^2) were stacked on the bottom section of the NC membrane. As mentioned above, the absorbent pad and buffer pad (grade 222) were attached to the adhesive side of a laminated card below the NC membrane. The position of other pads including the intermediate pad, ASPM, conjugate pad, and sample pad (Fusion 5) were fixed into a case that was created using a 3D printer (3Dison). The other structures for evaluating the components of the HEF-ICA were made of the same material and occupied the same position as in conventional ICA and HEF-ICA.

Kinetic analysis of antigen and AuNP conjugate release

For visualization of target antigen release from the sample pad, we utilized a DyLight 650-streptavidin (STA) conjugate as a reference. We loaded 2.5 μL of the DyLight 650-STA conjugate (500 $\mu\text{g mL}^{-1}$) onto the sample pad (fusion 5) in each structure, as described for the experiment presented in **Figure 2**. Thereafter, we loaded 120 μL of the buffered solution (1 \times PBS containing 10 mg mL^{-1} PVP and 5 mg mL^{-1} surfactant 10G) onto the buffer pad. We monitored the fluorescent signal in the detection zone using a ChemiDoc TM XRS⁺ imaging system (Bio-Rad Laboratories, Hercules, CA, USA). In case of the AuNP conjugate, the buffered solution was loaded onto the buffer pad. The color signal intensity was measured on the same analytical equipment. The captured image was analyzed using Image Lab 4.0 software (Bio-Rad). The colorimetric and fluorescence signal intensities were analyzed with the same pixel area in the captured image for each strip sensor, and the background signal intensity of the NC membrane was also analyzed using the same method. The subsequent signal intensity analyses were performed using the same method.

Measurement of diluted CRP

CRP was diluted with CRP-free serum from 0.01 $\mu\text{g mL}^{-1}$ to 500 $\mu\text{g mL}^{-1}$, for evaluating the hook effect and obtaining a titration curve. The diluted CRP solution was loaded onto the sample pad (grade 222): 120 μL for conventional ICA and 2.5 μL for HEF-ICA. In addition, 120 μL of the buffered solution was loaded onto the buffer pad in the case of HEF-ICA. The test and control line were analyzed using the

ChemiDoc TM XRS⁺ imaging system and Image Lab 4.0 software (Bio-Rad).

Evaluation of the HEF-ICA performance

The coefficient of variation (CV) was calculated as the standard deviation of signal intensities divided by the mean of the intensities for each concentration of CRP; assays were performed in triplicate. The assay time was determined as the time taken for the complete consumption of the AuNP conjugate, based on the results of the kinetic analysis of the AuNP conjugate. In case of application of the diluted sample on the conventional ICA, we diluted 2.5 μ L of the spiked CRP serum with 117.5 μ L of the buffered solution for use in the ICA (48 fold). The test and control line were also analyzed with the ChemiDoc TM XRS⁺ imaging system and Image Lab 4.0 software (Bio-Rad).

Measurement of CRP levels in clinical human serum samples

Human serum samples were obtained from the Kyungpook National University Chilgok Hospital in Korea. The study protocol was thoroughly explained to the patients and signed written informed consent was obtained in accordance with the approved guidelines and relevant regulations of the Institutional Review Board (KNUMC 2017-03-007-001). The serum samples were stored at -80 °C for subsequent analysis. The reference CRP levels were measured using a Hitachi 7180 analyzer (Hitachi, Japan). Quantification of CRP in human serum on the ICA strips was performed using the same procedure as described above.

Comparison of conventional ICA and HEF-ICA with the commercial kit for CRP

The commercial kit for CRP was purchased from Osang healthcare (Gyeonggi-do, Korea). We loaded 120 μ L of the diluted CRP solutions into the commercial kit. After 15 min, the signal intensity of the test and control line were analyzed with the ChemiDoc TM XRS⁺ imaging system and Image Lab 4.0 software (Bio-Rad).

Results and discussion

HEF-ICA structure, concept design, and operation

We speculated that the hook effect of conventional ICA results from a simultaneous reaction of excess target antigens with immobilized and labelled antibodies respectively. To prevent this reaction, HEF-ICA was designed, as shown in **Figure 1A**, for separation of migration time between the

target antigen and the AuNP conjugate. The sample pad is located in the middle of the strip as a bridge over the disconnected gap in the NC membrane. The delayed-release components, consisting of a stacked conjugate pad, ASPM, and intermediate pad, in that order, are located between the buffer and sample pad. The operation of the newly designed HEF-ICA strip is illustrated in **Figure 1B**. First, the sample solution is injected into the bridged sample pad and the buffered solution is injected into the buffer pad. The target protein in the sample solution migrates with the buffered solution and binds to the immobilized antibody on the test line. Next, unbound target protein is washed out and delayed-release components are moistened by the buffered solution during the migration of the sample. After the sample is wicked out, the AuNP conjugate is released from the conjugate pad. Finally, the sandwich immunoreaction is completed and the unbound AuNP conjugate is washed out to the absorbent pad. **Figure 1C** illustrates the differences in the migration flow of the immuno-components (target antigen, AuNP conjugate) on the NC membrane and the reaction mechanism on the test line between conventional ICA and HEF-ICA. In the case of conventional ICA, the target antigen preferentially cross-links with the labeled antibody. Unbound target antigens and the complex of target antigen and AuNP conjugate are mixed on the NC membrane and allowed to migrate to the immobilized antibody at the test line. As a result, the unbound excess target antigens inhibit the complex of target-antigen and AuNP conjugate from binding to the immobilized antibody. However, migration between the target antigen and AuNP conjugate are separated in HEF-ICA and an automatic washing process is included. This separation between the migration of the immuno-components and the additional automatic washing process eliminates the inhibitory effect of the unbound excess target antigens on the binding of the immobilized antibody. Consequently, a sequential sandwich immunoreaction occurs on the test line of HEF-ICA and the hook effect is eliminated. **Figure 1D** shows the estimated titration curve obtained as a result of the immune reaction in accordance with different CRP concentrations in conventional ICA and HEF-ICA. Conventional ICA yields a bell-shaped curve due to the hook effect at a high concentration of the target antigen. In contrast, HEF-ICA yields a signal intensity proportional to increasing target antigen concentrations, owing to elimination of the simultaneous reactions of the excess target antigens.

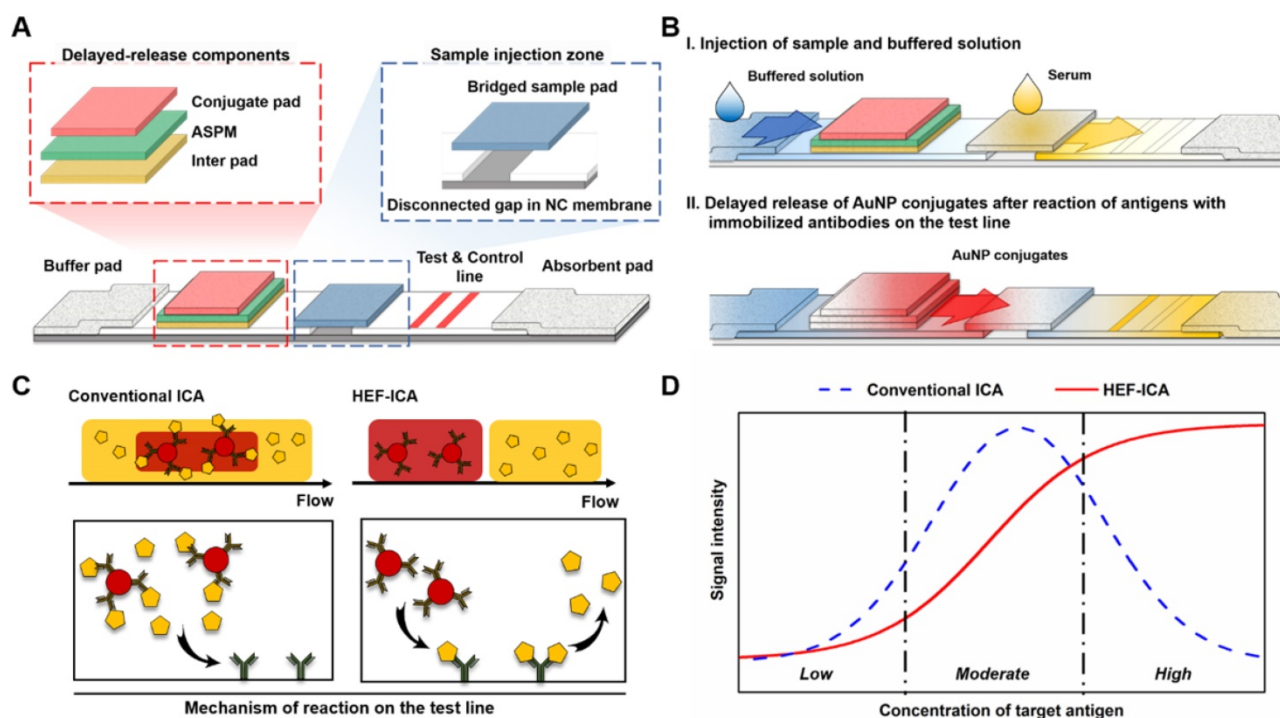


Figure 1. Schematic illustration of the hook effect-free immunochromatographic assay (HEF-ICA) (A), its operation mechanism (B), expected migration flow of the immuno-components and reaction mechanism on the test line compared with that in conventional ICA (C), and expected sandwich immunoreaction result of HEF-ICA compared with that of conventional ICA, according to concentration of the target protein (D).

Real-time release timing monitoring of a sample and AuNP conjugate for evaluation of the components of HEF-ICA

For evaluation of the newly developed components including the sample pad at a new location, disconnected gap in NC membrane, and the delayed-release components, we constructed progressive ICA structures (structure a: sample pad position; structure b: bridge sample pad; structure c: HEF-ICA), and evaluated time profiles of migration of the target antigen and AuNP conjugate in the detection zone (see **Figure 2**). The migration of the target antigen with time was analyzed using the STA-DyLight 650 conjugate to visualize the target antigen, and the fluorescent signal intensity was normalized. The AuNP conjugate was also analyzed by a colorimetric assay and normalized over time. Consequently, we confirmed the relative overlap ratio of AuNP conjugate with the target antigen in structures a, b, and c: 41.2%, 25.7%, and 5.2%, respectively, as shown by the marked area in each graph in **Figure 2**. This result clearly showed that ~95% of the AuNP conjugate migrated through the NC membrane without any mixing with the target antigen during the operation in case of the HEF-ICA structure (**Figure 2C**). The migration of the AuNP conjugate with a sample solution resulted in a 100% overlap of the AuNP conjugate with the target antigen in the case of conventional ICA (data not shown). We

also confirmed that the disconnected gap in the NC membrane and multilayered stacking of delayed-release components played a key role in the release timing separation between the target antigen and AuNP conjugate. The disconnected gap in the NC membrane and the bridging sample pad increased the release efficiency of the target antigens and AuNP conjugates. The mere stacking of the sample pad on the NC membrane divided the driving force of the buffered solution into the sample pad and NC membrane. However, the disconnected gap and bridging sample pad induced the entire transfer of the driving force of the buffered solution from the NC membrane to the sample pad and back to the NC membrane again. The resulting enhancement of the release efficiency of the target antigen was confirmed by comparing the time profile of the target antigen (closed square) in **Figure 2A-B**. Although the release efficiency of the target antigen decreased by combing delayed release components (**Figure 2C**), sufficient release of the target antigen was obtained for separation with migration of the AuNP conjugates. The additional paper materials (stacking of delayed-release components) showed much better performance than single ASPM stacking in terms of release uniformity and delayed release timing (see **Figure S1**). In particular, the intermediate pad diminishes the variation in the release of the AuNP conjugate, and we speculate that the difference in directional flow caused by the pore size of ASPM and

dispersion of the buffered solution in the intermediate pad increases the efficiency of delayed release of the AuNP conjugate [25]. The application of optimized delayed-release components significantly alters the migration of the AuNP conjugate in HEF-ICA as shown in **Figure 2C**. Consequently, the modification of the structure of HEF-ICA reduces the overlap between the target antigen and AuNP conjugate from 100% to 5.2%. We anticipated that the decline of this overlap would reduce the hook effect in HEF-ICA.

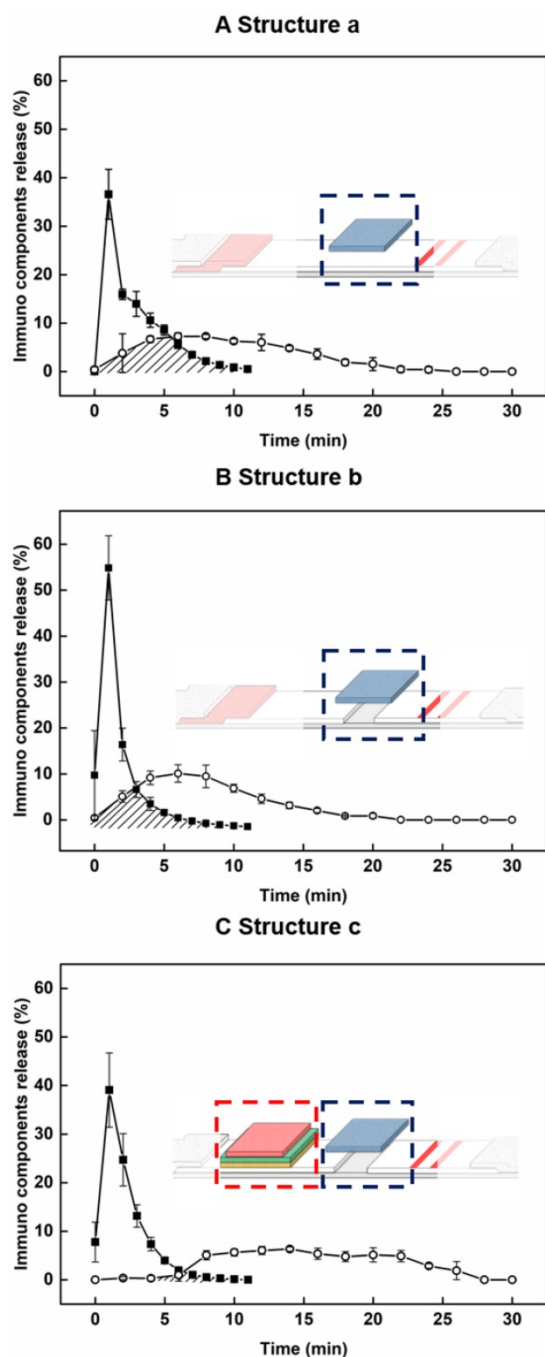


Figure 2. Time profiling of the proportion of AuNP conjugates (open circle) and target antigens (closed square) in each progressive modified structure. Structure a: application of sample pad position (**A**), Structure b: application of the disconnected gap in the NC membrane (**B**), Structure c: application of the delayed release components (**C**).

Adjustment of the titration curve of HEF-ICA with the Hill equation and evaluation of HEF-ICA performance

The performance of HEF-ICA was compared with that of a conventional ICA using CRP-free serum spiked with $0.01 \mu\text{g mL}^{-1}$ to $500 \mu\text{g mL}^{-1}$ of CRP (**Figure 3**). The titration curve of conventional ICA declined starting from $1 \mu\text{g mL}^{-1}$; however, the titration curve of HEF-ICA showed an increasing trend up to $100 \mu\text{g mL}^{-1}$ and a saturation range over $100 \mu\text{g mL}^{-1}$. HEF-ICA has a nonlinear titration curve due to saturation at a high concentration of the target antigen. We expected that the titration curve would be similar to that of an ELISA because the reaction mechanism of HEF-ICA is similar to that of ELISA owing to preferential cross-linking of the target antigen with the immobilized antibody rather than the labeled antibody [26]. Based on adjustment with the Hill model equation, as shown in **Figure 4**, we obtained well-correlated results ($R^2 = 0.99$). After adjusting the titration curve with the Hill equation, we quantified the CRP concentration. The limit of detection (LOD) was calculated at a concentration of signal intensity $3\times$ that of the control in HEF-ICA, and the dynamic range was determined from the limit of quantitation (LOQ), which was calculated at $5\times$ the signal intensity, to the saturation point. The parameters of the Hill equation were calculated as follows: $n = 1.13 \pm 0.2$, $k = 3.56 \pm 0.86$, and $I_{\text{Max}} = 11740 \pm 394$ a.u. The coefficient of variation (CV), which was evaluated for each concentration of CRP, was within a suitable range ($\sim 10\%$) of the proportional range in conventional ICA and HEF-ICA, as shown in **Figure S2**. The proportional range was determined as follows: $0.01\text{--}1 \mu\text{g mL}^{-1}$ (conventional ICA), $0.1\text{--}500 \mu\text{g mL}^{-1}$ (HEF-ICA). A relatively high CV value was obtained in the range of the hook effect in conventional ICA. The assay time of both structures was determined as the time taken for the consumption of the total AuNP conjugates and for washing out in order to reduce interference of the colorimetric signal of the test line. Therefore, we monitored the migration of AuNP conjugates on the NC membrane by time, as shown **Figure S3**. Based on the time profiling of migration of AuNP conjugates, we evaluated the assay time for each structure. The calculated specification of HEF-ICA in comparison with that of conventional ICA has been summarized in **Table 1**.

The comparison between HEF-ICA and conventional ICA revealed that HEF-ICA has lower sensitivity than the conventional ICA. We assumed that the difference in sensitivity originates from the difference in injected sample volume. In order to confirm this, the titration curve was modified by

plotting the signal intensity for conventional ICA and HEF-ICA based on the quantity of CRP, as shown in **Figure S4**. The plots showed a similar trend and proportional range, regardless of structure. The finding suggests that the affinity of antibodies is maintained in HEF-ICA, and the lower sensitivity is attributable to the injected sample volume. Additionally, we calculated the limit of detection of CRP quantity with respect to injected sample volume. The limit of detection in conventional ICA is 0.533 ng, while that of HEF-ICA was 1.08 ng. We speculated that the difference is attributable to the reaction time of the target antigens. In HEF-ICA, target antigens react with the immobilized antibodies for about 7 min. However, the reaction time of the target antigen in the conventional ICA was the total assay time (about 18 min). Based on the reaction time of target antigens, the binding efficiency of conventional ICA was found to be higher than that of HEF-ICA; however, the difference was not significant.

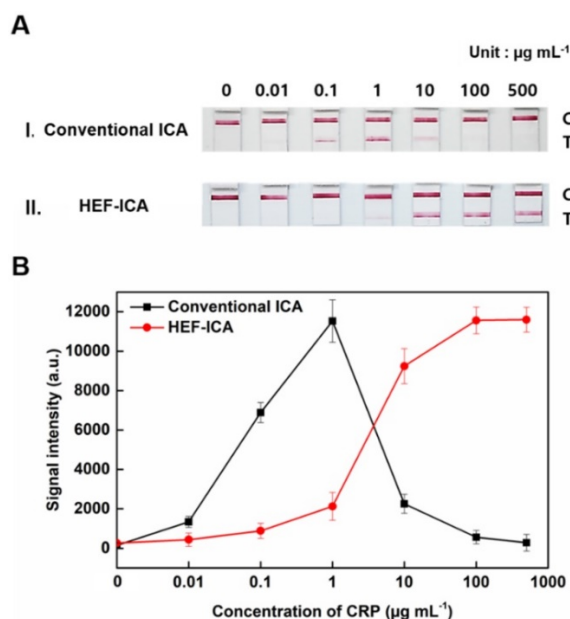


Figure 3. Comparison between HEF-ICA and conventional ICA performance (A). Titration curve (B).

Table 1. Comparison of the performance of conventional ICA and HEF-ICA.

| | Conventional ICA | HEF-ICA |
|------------------------|--|---|
| LOD | 4.1 ng mL ⁻¹ | 43 ng mL ⁻¹ |
| Dynamic range | 19 ng mL ⁻¹ ~ 1 µg mL ⁻¹ | 119 ng mL ⁻¹ ~ 100 µg mL ⁻¹ |
| Assay time | 18 min | 23 min |
| Initial process step | One step | Two steps |
| Required sample volume | 120 µL | 2.5 µL |
| Hook Effect | Occurrence (> 1 µg mL ⁻¹) | Non-Occurrence (Saturation point: > 100 µg mL ⁻¹) |

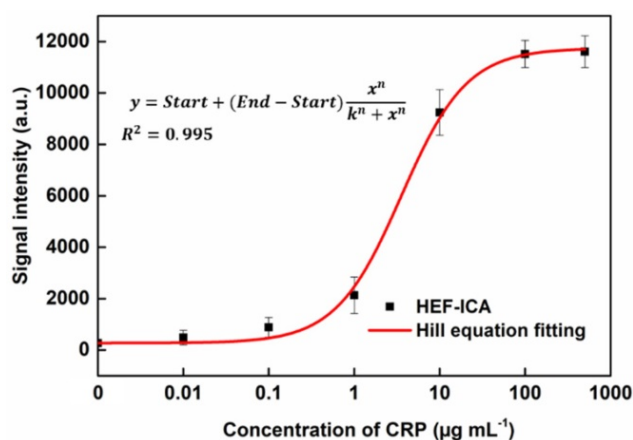


Figure 4. Adjustment of the titration curve with the Hill equation for HEF-ICA.

The sample volume of HEF-ICA was reduced because of the risk of contact between the sample solution and the delayed-release components. Therefore, we minimized the injection sample volume in HEF-ICA to 2.5 µL. Further, as the lower injection sample volume may result in significantly low sensitivity, sample volumes of less than 2.5 µL were not considered. These lower sample volumes reduce the hook effect in ICA; accordingly, we examined the effect of the minimized sample volume on the conventional ICA assay using a diluted sample, where the amount of undiluted sample was equal to that used for HEF-ICA. As shown in **Figure S5**, the titration curve of conventional ICA using the diluted sample was similar to that of HEF-ICA in the proportional range. However, the hook effect occurred at higher concentrations of CRP than 100 µg mL⁻¹, and a relatively high LOD was observed (0.139 µg mL⁻¹) when the conventional ICA was performed using a diluted sample. We summarized the specifications by structure and sample dilution in **Table S1**. The dynamic range was evaluated by dividing the concentration of the upper limit by that of the lower limit. On comparing the value, the dilution of the sample solution in the conventional ICA was found to broaden the dynamic range; however, that of HEF-ICA was broader despite the use of undiluted sample.

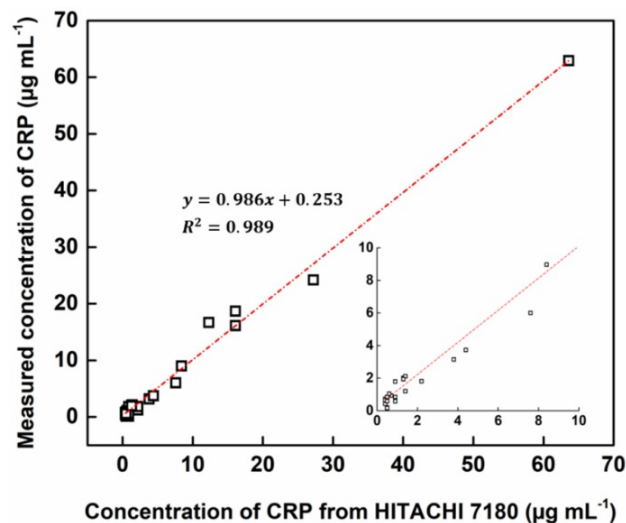
Additionally, we summarized and compared the specification of HEF-ICA with the previously established ICA overcoming the hook effect, as shown in **Table 2**. Although the assay time for HEF-ICA was relatively long, the lack of requirement of a sample preparation step compensated for this. The elimination of the hook effect and requirement of a very small injection volume of the sample are highly useful considerations for its efficiency as a POCT.

Table 2. Comparison of the specification of HEF-ICA with the previously established ICA in terms of elimination of the hook effect.

| Reference | Limit of detection (LOD) | Dynamic range | Assay time | Solution injection | Strategy for hook effect |
|-----------|----------------------------|--|------------|--|---|
| [23] | Semi-quantitative analysis | Distinction of several concentration range section | 20 min | 100 μL (serum/plasma) or 120 μL (blood) | Additional test line |
| [24] | Not specified | Not specified | 2 min | 40 μL diluted serum and 60 μL running buffer | Kinetic analysis between test and control line |
| [25] | 0.649 ng mL^{-1} | 0.67 ng mL^{-1} - 1.02 mg mL^{-1} | 10min | Not specified | Additional test line and data analysis |
| This work | 43 ng mL^{-1} | 119 ng mL^{-1} - 100 $\mu\text{g mL}^{-1}$ Saturation range: >100 $\mu\text{g mL}^{-1}$ | 23 min | 2.5 μL serum and 120 μL running buffer | Alteration of assay mechanism by modified structure |

Furthermore, we compared the conventional ICA and HEF-ICA with a commercial ICA for CRP. In accordance with the product manual, the titration curve was obtained using diluted serum sample, as shown in **Figure S6**. The hook effect also occurred at concentrations higher than 100 $\mu\text{g mL}^{-1}$ for the commercial ICA for CRP, likewise for the conventional ICA, despite dilution of the sample. Moreover, commercial ICA for CRP is divided into CRP and high-sensitivity CRP (hs-CRP) detection, because it is difficult to measure the wide range of CRP at the same time. On the other hand, the dynamic measurement range of HEF-ICA fully covered the physiological range of CRP in human serum without sample dilution.

These results indicate that HEF-ICA shows high potential for application as a POCT, owing to its wide dynamic range and requirement for only small amounts of undiluted sample volume, and elimination of the hook effect. We anticipate that HEF-ICA should enhance the practicality of the ICA as a POCT.

**Figure 5.** Accuracy testing for 33 clinical samples in comparison with that of a clinical chemistry analyzer.

Evaluation of clinical samples

Using HEF-ICA, we analyzed 33 undiluted clinical serum samples and quantified CRP concentrations. The HEF-ICA measurement results were compared with those obtained using a clinical chemistry analyzer. As shown in **Figure 5**, the value of the coefficient of determination (0.98) was high within the range of CRP concentrations of 0.2 $\mu\text{g mL}^{-1}$ to 63.6 $\mu\text{g mL}^{-1}$. Although we did not evaluate the complete range of CRP levels, accuracy and practicality were confirmed for the possible commercialization of HEF-ICA as a POCT to detect a wide range of CRP levels without the hook effect and requirement for sample preparation.

Conclusion

We developed the present HEF-ICA for the detection of a wide range of CRP concentrations via direct quantitative measurement. The migration of the target antigen and the AuNP conjugate was efficiently separated by means of the bridged sample pad and delayed-release components. This separation induced an automatic washing step within the reaction of the target antigen and AuNP conjugate. Further, this separation minimized the simultaneous reaction of the excess target antigens with both antibodies, thereby resulting in a signal intensity proportional to increasing concentrations of CRP. We further adjusted the titration curve of HEF-ICA with the Hill equation for quantitative analysis, and evaluated the performance of HEF-ICA. The LOD was obtained as 43 ng mL^{-1} , with a dynamic range from 119 ng mL^{-1} to 100 $\mu\text{g mL}^{-1}$ and a saturation range over 100 $\mu\text{g mL}^{-1}$. The evaluated sensitivity of HEF-ICA is lower than that of conventional ICA; therefore, HEF-ICA is not suitable for use with biomarkers that require detection with high sensitivity. However, for certain biomarkers, such as CRP, HCG, and PSA (prostate specific antigen), a wide range of concentrations, rather than high sensitivity, is more important [27, 28]. For these biomarkers, HEF-ICA is adequate and more practical as a POCT biosensor. Although the

initial processing step and assay time of HEF-ICA are drawbacks in comparison with conventional ICA, these issues are compensated for by the circumvention of the hook effect in the former and commercial ICA for CRP. Further, HEF-ICA offers practical advantages such as the requirement for a small sample volume (less than one droplet), lack of requirement for the sample preparation process, and measurement of a wide range of concentrations of a target antigen without the hook effect. The accuracy of HEF-ICA was also evaluated via application of clinical samples whose CRP concentration had been measured using a clinical chemistry analyzer. In particular, as required small sample volumes may be obtained via fingertip blood sampling using a lancet, it is more suitable for POCT. Additionally, the operation of HEF-ICA with a buffered solution and small sample volume could reduce the matrix effect of the sample, thus affording applicability to various types of samples.

Abbreviations

Ab: antibody; ASPM: asymmetric polysulfone membrane; AuNP: gold nanoparticle; BSA: bovine serum albumin; CRP: C-reactive protein; CV: coefficient of variation; ELISA: enzyme-linked immunosorbent assay; HEF-ICA: hook effect-free immunochromatographic assay; ICA: immunochromatographic assay; LOD: limit of detection; LOQ: limit of quantitation; NC membrane: nitrocellulose membrane; PBS: phosphate-buffered saline; POCT: point-of-care test; PSA: prostate specific antigen; PVP: polyvinylpyrrolidone.

Supplementary Material

Supplementary figures and tables.
<http://www.thno.org/v08p3189s1.pdf>

Acknowledgement

This work was financially supported by grants from the Mid-career Researcher Program (NRF-2017R1A2B3010816) through National Research Foundation grant funded by the Ministry of Science, ICT and Future Planning, by the R&D Program for Society of the National Research Foundation (NRF) funded by the Ministry of Science, ICT & Future Planning (2015M3A9E2031375) and by the Original Technology Research Program for Brain Science through the National Research Foundation of Korea (NRF) (NRF-2015M3C7A1029196).

Competing Interests

The authors have declared that no competing interest exists.

References

1. Ablij H, Meinders A. C-reactive protein: history and revival. *Eur J Intern Med.* 2002; 13: 412.
2. Du Clos TW. Function of C-reactive protein. *Ann Med.* 2000; 32: 274-8.
3. Pearson TA, Mensah GA, Alexander RW, Anderson JL, Cannon RO, 3rd, Criqui M, et al. Markers of inflammation and cardiovascular disease: application to clinical and public health practice: A statement for healthcare professionals from the Centers for Disease Control and Prevention and the American Heart Association. *Circulation.* 2003; 107: 499-511.
4. Clyne B, Olshaker JS. The C-reactive protein. *J Emerg Med.* 1999; 17: 1019-25.
5. Lau B, Sharrett AR, Kingsley LA, Post W, Palella FJ, Visscher B, et al. C-reactive protein is a marker for human immunodeficiency virus disease progression. *Arch Intern Med.* 2006; 166: 64-70.
6. Ledue TB, Rifai N. Preanalytic and analytic sources of variations in C-reactive protein measurement: implications for cardiovascular disease risk assessment. *Clin Chem.* 2003; 49: 1258-71.
7. Horiuchi M, Mogi M. C-reactive protein beyond biomarker of inflammation in metabolic syndrome. *Hypertension.* 2011; 57: 672-3.
8. Libby P, Ridker PM. Inflammation and atherosclerosis: role of C-reactive protein in risk assessment. *Am J Med.* 2004; 116(Suppl 6A): 9-16.
9. Ridker PM. Clinical application of C-reactive protein for cardiovascular disease detection and prevention. *Circulation.* 2003; 107: 363-9.
10. Ridker PM, Rifai N, Clearfield M, Downs JR, Weis SE, Miles JS, et al. Measurement of C-reactive protein for the targeting of statin therapy in the primary prevention of acute coronary events. *N Engl J Med.* 2001; 344: 1959-65.
11. Rodriguez-Moran M, Guerrero-Romero F. Increased levels of C-reactive protein in noncontrolled type II diabetic subjects. *J Diabetes Complications.* 1999; 13: 211-5.
12. Coelho L, Povoia P, Almeida E, Fernandes A, Mealha R, Moreira P, et al. Usefulness of C-reactive protein in monitoring the severe community-acquired pneumonia clinical course. *Crit Care.* 2007; 11: R92.
13. Koenig W, Sund M, Frohlich M, Fischer HG, Lowel H, Doring A, et al. C-Reactive protein, a sensitive marker of inflammation, predicts future risk of coronary heart disease in initially healthy middle-aged men: results from the MONICA (Monitoring Trends and Determinants in Cardiovascular Disease) Augsburg Cohort Study, 1984 to 1992. *Circulation.* 1999; 99: 237-42.
14. Ridker PM, Cannon CP, Morrow D, Rifai N, Rose LM, McCabe CH, et al. C-reactive protein levels and outcomes after statin therapy. *N Engl J Med.* 2005; 352: 20-8.
15. Vashist SK, Venkatesh AG, Marion Schneider E, Beaudoin C, Luppia PB, Luong JH. Bioanalytical advances in assays for C-reactive protein. *Biotechnol Adv.* 2016; 34: 272-90.
16. Bryan T, Luo X, Bueno PR, Davis JJ. An optimised electrochemical biosensor for the label-free detection of C-reactive protein in blood. *Biosens Bioelectron.* 2013; 39: 94-8.
17. Gupta RK, Periyakaruppan A, Meyyappan M, Koehne JE. Label-free detection of C-reactive protein using a carbon nanofiber based biosensor. *Biosens Bioelectron.* 2014; 59: 112-9.
18. Zhang P, Bao Y, Draz MS, Lu H, Liu C, Han H. Rapid and quantitative detection of C-reactive protein based on quantum dots and immunofiltration assay. *Int J Nanomedicine.* 2015; 10: 6161-73.
19. Lin SC, Tseng CY, Lai PL, Hsu MY, Chu SY, Tseng FG, et al. Paper-based CRP Monitoring Devices. *Sci Rep.* 2016; 6: 38171.
20. Posthuma-Trumpie GA, Korf J, van Amerongen A. Lateral flow (immuno)assay: its strengths, weaknesses, opportunities and threats. A literature surveys. *Anal Bioanal Chem.* 2009; 393: 569-82.
21. Tate J, Ward G. Interferences in immunoassay. *Clin Biochem Rev.* 2004; 25: 105-20.
22. Leung W, Chan CP, Rainer TH, Ip M, Cautherley GW, Renneberg R. InfectCheck CRP barcode-style lateral flow assay for semi-quantitative detection of C-reactive protein in distinguishing between bacterial and viral infections. *J Immunol Methods.* 2008; 336: 30-6.
23. Rey EG, O'Dell D, Mehta S, Erickson D. Mitigating the Hook Effect in Lateral Flow Sandwich Immunoassays Using Real-Time Reaction Kinetics. *Anal Chem.* 2017; 89: 5095-100.
24. Oh YK, Joung HA, Han HS, Suk HJ, Kim MG. A three-line lateral flow assay strip for the measurement of C-reactive protein covering a broad physiological concentration range in human sera. *Biosens Bioelectron.* 2014; 61: 285-9.
25. Joung HA, Oh YK, Kim MG. An automatic enzyme immunoassay based on a chemiluminescent lateral flow immunosensor. *Biosens Bioelectron.* 2014; 53: 330-5.
26. Cheng CM, Martinez AW, Gong J, Mace CR, Phillips ST, Carrilho E, et al. Paper-based ELISA. *Angew Chem Int Ed Engl.* 2010; 49: 4771-4.
27. Gronowski AM, Cervinski M, Stenman UH, Woodworth A, Ashby L, Scott MG. False-negative results in point-of-care qualitative human chorionic gonadotropin (hCG) devices due to excess hCGbeta core fragment. *Clin Chem.* 2009; 55: 1389-94.
28. Vaidya HC, Wolf BA, Garrett N, Catalona WJ, Clayman RV, Nahm MH. Extremely high values of prostate-specific antigen in patients with adenocarcinoma of the prostate: demonstration of the "hook effect". *Clin Chem.* 1988; 34: 2175-7.